

See discussions, stats, and author profiles for this publication at: <https://www.researchgate.net/publication/277141214>

Analyse LIBS de légumes

Conference Paper · May 2009

CITATIONS

0

READS

81

7 authors, including:



Sid Ahmed Beldjilali

Université des Sciences et de la Technologie d'Oran Mohamed Boudiaf

45 PUBLICATIONS 134 CITATIONS

[SEE PROFILE](#)



Laurent Mercadier

European XFEL

49 PUBLICATIONS 311 CITATIONS

[SEE PROFILE](#)



Jin Yu

Shanghai Jiao Tong University

108 PUBLICATIONS 2,726 CITATIONS

[SEE PROFILE](#)

Some of the authors of this publication are also working on these related projects:



Teramobile [View project](#)



Quality control of food by laser-induced breakdown spectroscopy [View project](#)



Evaluation of minor element concentrations in potatoes using laser-induced breakdown spectroscopy[☆]

S. Beldjilali^{a,b}, D. Borivent^a, L. Mercadier^a, E. Mothe^a, G. Clair^c, J. Hermann^{a,*}

^a LP3, CNRS-Université d'Aix Marseille II, 163 Av. de Luminy, 13288 Marseille, France

^b LPPMCA, Université des Sciences et de la Technologie d'Oran, BP 1505 El Mnaouer, Oran, Algeria

^c CEA Saclay, DEN/DANS/DPC/SCP/LRSI, 91191 Gif-sur-Yvette, France

ARTICLE INFO

Article history:

Received 2 December 2009

Accepted 18 April 2010

Available online 24 April 2010

Keywords:

Laser plasma

Plasma modeling

Calibration-free LIBS

Quality control of aliments

ABSTRACT

We have performed spectroscopic analysis of the plasma generated by Nd:YAG laser irradiation of flesh and skin of fresh potatoes. From the spectra recorded with an Echelle spectrometer 11 minor elements have been identified. Their relative concentrations were estimated by comparing the measured spectra to the spectral radiance computed for a plasma in local thermal equilibrium. According the moderate plasma temperature of about 6500 K at the time of spectroscopic observation, the electrons are essentially generated by the ionization of the minor metal atoms, making plasma modeling possible although the organic elements may be out of equilibrium. Among the spectral lines selected for the analysis, the Na I 588.99 and 589.59 nm doublet was found to be partially self-absorbed allowing us to estimate the number density of sodium atoms. The value was found to agree with the number density predicted by the plasma model. As a result, the relative concentrations of the detected minor elements have been estimated for both the flesh and skin of the potatoes. Among these, aluminum and silicon were found to have relatively large mass fractions in the potato skin whereas their presence was not detected in the flesh. The present study shows that laser-induced breakdown spectroscopy is a promising tool to measure the elemental composition of fresh vegetables without any sample preparation.

© 2010 Elsevier B.V. All rights reserved.

1. Introduction

The control of minor element concentrations in food is necessary to evaluate sanitary risks. Several studies have shown a correlation between health problems and exposure to specific substances [1]. The detection of salutary and harmful elements in aliments such as fresh vegetables or fruits can provide useful assessment and control for safe and healthy alimentation [2]. Toxic elements such as heavy metals found in agricultural products may lead to intoxication and also, with prolonged accumulation, neurodegenerative diseases [3].

During the past years, several crises in the food chain, such as the mad cow disease, and the dioxin-contaminated chicken, demonstrated that fast tools for alimental analysis are required. For this purpose, different techniques such as flame atomic absorption spectrometry (FAAS) [4–6] or graphite furnace atomic absorption spectrometry (GFAAS) [7,8], inductively coupled atomic emission spectroscopy (ICP-AES) [9] and inductively coupled plasma mass spectrometry

(ICP-MS) [10,11] or laser-induced breakdown spectroscopy (LIBS) [12] have been proposed. Compared to conventional techniques such as ICP or AAS, LIBS has some distinct advantages [13]: it allows for realtime and stand-off analysis of multielemental samples and does not require any sample preparation. In addition, by choosing the appropriate irradiation conditions (laser wavelength, pulse duration, pulse energy and focalization geometry) LIBS may be applied to analyze every kind of material, independently of its chemical composition. As a result of the recent progress in the technologies of laser sources, compact spectrometers and detectors, reliable portable LIBS systems are now available, ensuring new applications of LIBS analysis in fields such as environmental survey and quality control of aliments [14]. LIBS is also promising for applications in many other fields such as interplanetary exploration [15], quality control in industrial production [16], recycling of materials and analyses in hazardous and dangerous environments [17].

However, quantitative LIBS analyses are generally limited to inorganic samples [18,19] because of the matrix effect: the properties of the laser-produced plasma depend critically on the sample composition. In case of complex organic materials such as fresh vegetables or other ailments, the measurement calibration is inefficient. To overcome this difficulty, we investigate in the present study a quantitative measurement procedure based on the comparison of the measured spectrum to the spectral radiance computed for

[☆] This paper was presented at the 5th Euro-Mediterranean Symposium on Laser Induced Breakdown Spectroscopy, held in Tivoli Terme (Rome), Italy, 28 September–1 October 2009, and is published in the Special Issue of Spectrochimica Acta Part B, dedicated to that Symposium.

* Corresponding author. Tel.: +33 4 9182 9290.

E-mail address: hermann@lp3.univ-mrs.fr (J. Hermann).

a plasma in local thermal equilibrium (LTE). The procedure was patented by the French National Centre of Scientific Research (CNRS) [20].

2. Experimental set-up

Material ablation was produced by an Nd:YAG laser (Quantel, model Brio) that was operated at 1064 nm. The laser delivered pulses of 100-mJ energy and 4-ns duration at a repetition rate of 20 Hz. The experimental apparatus is schematized in Fig. 1. The laser pulse energy was reduced to 10 mJ by turning the beam polarization with the aid of a half-wave plate and crossing through a polarization analyzer. The laser beam was focused onto the sample surface in the vertical direction using a plano-convex lens of 150-mm focal length. According to a spot diameter of about 120 μm , a laser fluence of about 50 J cm^{-2} was obtained on the sample surface. The samples were prepared from fresh potatoes by cutting square cuboids of 10²-mm² surface and 5-mm height. They were placed on a motorized target holder allowing for computer-controlled translation in the three orthogonal directions. In case of analysis of the potato skin, the surface was not completely flat and only a limited area of about 4 mm² was scanned during the measurements. To capture the plasma emission, the plume was imaged onto the entrance of an optical fiber of 600- μm diameter using two lenses of 150- and 35-mm focal lengths. The fiber was coupled to the entrance of an Echelle spectrometer (LTB, model Aryelle Butterfly) of 0.4-m focal length and a spectral resolution $\lambda/\Delta\lambda \approx 1 \times 10^4$. Photon detection was ensured using an intensified charge-coupled device (ICCD) matrix detector (Andor, model model IStar). An intensity calibration of the spectroscopic apparatus has been performed in the visible and UV spectral ranges using a calibrated tungsten lamp (Oriel, model 63358) and a deuterium lamp (Heraeus, model DO544J), respectively. The spectral width of the apparatus was measured as a function of wavelength using a low pressure mercury lamp.

The spectroscopic measurements of the laser-produced plasma were performed with an observation gate of 5 μs duration that was delayed by 1 μs with respect to the laser pulse. To enhance the signal-to-noise ratio, data acquisition was performed by averaging over 50 ablation events on different irradiation sites. The sites were separated by a distance of 250 μm . The experimental procedure was controlled via a controller unit (Newport, model XPS) and appropriate software.

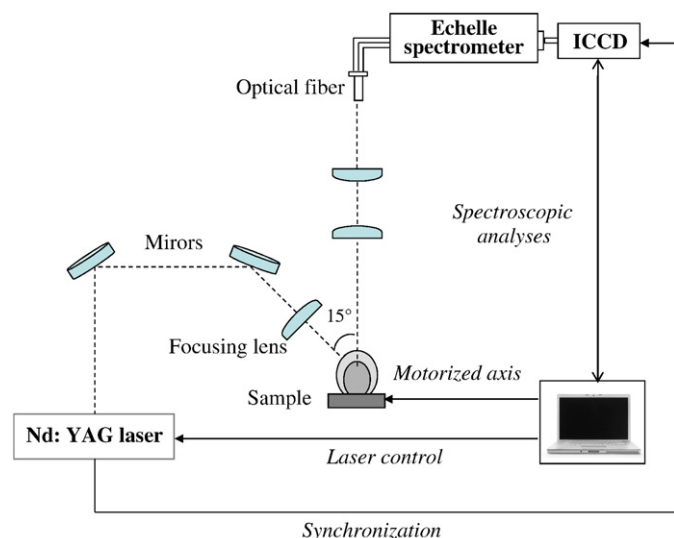


Fig. 1. Schematic presentation of the experimental set-up.

3. Results and discussion

3.1. Spectroscopic database

The spectral lines that have been selected for the present analysis are listed in Table 1. They belong to neutral atoms of 14 different elements including carbon, hydrogen, oxygen and 11 minor elements. The spectral lines have been chosen to measure plasma temperature, electron density and the relative elemental concentrations. Only spectral lines of neutral atoms were considered in order to simplify the data analyses. Indeed, metals have similar ionization potentials (see Table 1) and the radiation from the corresponding neutral atoms is expected to be emitted from the same plasma volume. Contrarily, the ionic species mainly radiate from the volume of large temperature. Thus, temperature gradients have to be taken into account if spectral line emission from both neutral atoms and ions is considered.

Spectral lines of known Stark broadening coefficients have been chosen in priority in order to take into account self-absorption. Most of the transitions were found to be optically thin. Contrarily, significant self-absorption of the sodium resonance lines Na I 588.99 and 589.59 nm was evidenced. Thus, the number densities of Na ground state neutral atoms could be deduced from the relative intensities of both spectral lines.

Table 1

Radiative decay A_{ul} , energy E and statistical weight g of upper (index u) and lower (index l) excitation levels, and Stark width w and shift d for $n_e = 1 \times 10^{17} \text{ cm}^{-3}$ of the selected transitions.

Transition	$A_{ul} (\text{s}^{-1})$	$E_l (\text{cm}^{-1})$	g_l	$E_u (\text{cm}^{-1})$	g_u	$w (\text{pm})$	$d (\text{pm})$
H I 656.28	1.323 10 ⁸ ^a	82259	4	97492	6	850	0.5
C I 247.86	1.8 10 ¹⁷ ^b	21648	1	61982	3	6.9 ^m	4.4 ^m
O I 777.42	3.293 10 ⁷ ^c	73768	5	86628	5	–	–
Mg I 383.83	1.594 10 ⁸ ^d	21911	5	47957	7	110 ^m	–2 ^m
Mg I 516.73	1.130 10 ⁷ ^e	21850	1	41197	3	33 ^m	9 ^m
Mg I 517.27	3.370 10 ⁷ ^e	21870	3	41197	3	35 ^m	8.4 ^m
Mg I 518.36	5.464 10 ⁷ ^e	21911	5	41197	3	35 ^m	7.4 ^m
Al I 394.40	5.105 10 ⁷ ^f	0	2	25348	2	34 ⁿ	17 ⁿ
Al I 396.15	1.010 10 ⁸ ^f	122	4	25348	2	34 ⁿ	17 ⁿ
Ca I 431.86	7.38 10 ⁷ ^g	15316	5	38465	3	16 ^o	–
Fe I 300.05	6.027 10 ⁶ ^h	11976	9	45295	11	–	–
Fe I 404.58	8.622 10 ⁷ ⁱ	11976	9	36686	9	–	–
Na I 588.99	6.289 10 ⁷ ^g	0	2	16973	4	75 ^p	11 ^p
Na I 589.59	6.277 10 ⁷ ^g	0	2	16956	2	65 ^p	12 ^p
Mn I 403.08	1.738 10 ⁷ ^j	0	6	24802	8	57 ^m	–
Ti I 498.17	6.594 10 ⁷ ^j	6843	11	26911	13	–	–
Li I 670.77	3.721 10 ⁷ ^c	0	2	14904	4	–	–
Si I 251.43	6.108 10 ⁷ ^k	0	1	39760	3	30 ^o	7 ^o
Si I 251.61	1.212 10 ⁸ ^k	223	5	39955	5	30 ^o	6 ^o
Si I 251.92	4.510 10 ⁷ ^k	77	3	39760	3	28 ^o	6 ^o
Si I 252.41	1.818 10 ⁸ ^k	77	3	39683	1	28 ^o	7 ^o
K I 769.90	3.802 10 ⁷ ^g	0	2	12985	2	(5)	(4)
Cu I 324.75	1.370 10 ⁸ ^l	0	2	30784	4	14 ^r	–

^a Ref. [21].

^b Ref. [22].

^c Ref. [23].

^d Ref. [24].

^e Ref. [25].

^f Ref. [26].

^g Ref. [27].

^h Ref. [28].

ⁱ Ref. [29].

^j Ref. [30].

^k Ref. [31].

^l Ref. [32].

^m Ref. [33].

ⁿ Ref. [34].

^o Ref. [35].

^p Ref. [36].

^r Ref. [37].

3.2. Calculation of the spectral radiance

The calculation of the spectral radiance is divided into three successive steps as illustrated in Fig. 2. (i) The first step deals with the calculation of the plasma composition. (ii) In the second step, the absorption coefficient is computed as a function of wavelength, taking into account the dominating effects of spectral line broadening. (iii) The spectral radiance of the plasma is calculated in the third step using a simplified solution of the radiation transport equation. The computed spectrum is then compared to the experimental one. Plasma temperature, electron density and the relative concentrations of the different elements are adjusted to obtain the best agreement between measured and calculated spectra. The comparison concerns the intensity and the spectral width of the spectral lines that were chosen for the analysis (see Table 1).

- (i) The composition of a plasma in LTE is determined by the temperature T and the atomic number densities of elements. In the temperature range of interest ($T \approx 10^4$ K), the presence of molecules in the plasma can be neglected. Details on the calculation algorithm that was applied to compute the plasma composition can be found in a previous paper [38]. As an example, the number densities of species in a LTE plasma of an elemental composition typical of a potato are displayed in Fig. 3 versus temperature. It is shown that the electrons are essentially due to the ionization of metal atoms for $T < 8000$ K whereas the contribution of organic atoms ionization dominates at larger temperatures.
- (ii) The absorption coefficient as a function of wavelength is calculated for each spectral line using [39]

$$\alpha(\lambda) = \pi r_0^2 \lambda^2 f_{lu} n_l P(\lambda) \left[1 - \exp\left(-\frac{hc}{\lambda kT}\right) \right] \quad (1)$$

where r_0 is the classical electron radius, c the vacuum light velocity, f_{lu} and n_l are the absorption oscillator strength and the lower level population density of the transition, respectively. The normalized line profile $P(\lambda)$ is calculated considering Doppler and Stark broadening that are the dominant mechanisms of spectral line broadening in strongly ionized laser-produced plasmas [40]. Depending on the relative values of Doppler and Stark width, the line shape is described by a

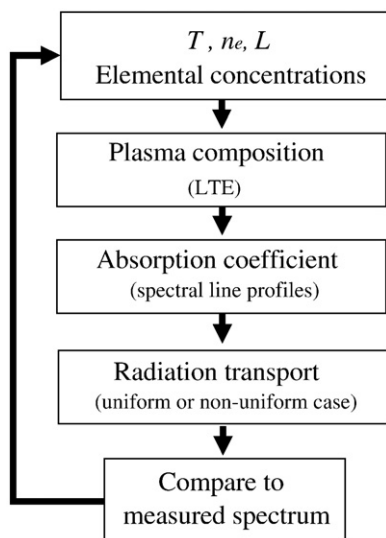


Fig. 2. Schematic presentation of the calculation loop. Temperature, electron density and elemental concentrations are deduced by comparing the computed spectral radiance to the measured spectrum.

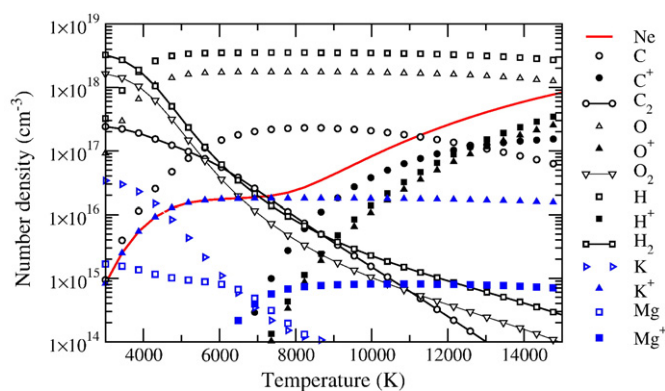


Fig. 3. Number densities of species versus temperature computed for a plasma in local thermal equilibrium of an elemental composition typical for a potato. The pressure was set to a constant value of 5×10^3 Pa. Only species of the two most abundant metals K and Mg are presented. It is shown that the electrons are essentially generated by the ionization of metal atoms for $T < 8000$ K.

Gaussian, a Lorentzian or a Voigt profile. The Doppler width is calculated according to plasma temperature and atomic mass of the emitting species, the Stark width is estimated for each spectral line of interest assuming a linear increase with electron density.

- (iii) The spectral radiance is calculated using an analytical solution of the radiation transport equation for a uniform plasma in local thermal equilibrium.

$$B_\lambda = U_\lambda(T) \left(1 - e^{-\alpha(\lambda, T)L} \right) \quad (2)$$

Here, U_λ is the blackbody spectral radiance and L is the plasma dimension in the observation direction.

3.3. Temperature and electron density measurements

The plasma temperature was measured using spectral lines of magnesium that is present in all vegetables with relative large concentrations (see Table 2). Thus, several spectral lines emitted from two multiplets of significant different excitation energies can be observed as shown in Fig. 4. We deduce for the plasma produced by the irradiation of both the potato flesh and skin a temperature $T = 6500$ K.

A first estimation of the electron density is performed using the Stark broadening effect of the Hydrogen Balmer line at 656.28 nm (see Fig. 5). The H_α transition is easily observed in plasmas produced by laser ablation of fresh vegetables due to the large water content. Comparing the measured and computed spectral line profiles, we deduce electron density values of about 2.7×10^{16} and $2.2 \times 10^{16} \text{ cm}^{-3}$ for potato flesh and skin, respectively.

It is however noted, that the electron density deduced from the Stark broadening of the H_α transition is expected to be larger than the n_e -value deduced from the spectral lines of minor elements. In fact, the plasma emission is acquired over a duration of 5 μs during which the plasma temperature decreases. As the Hydrogen Balmer line has a large excitation energy (see Table 1), its significant emission is limited to a short duration during the early stage of plume expansion when the temperature was high. The measured spectral line width corresponds therefore to the early expansion stage where the electron density was relatively large. Contrarily, the observed transitions of the minor elements have much smaller excitation energies. Thus, the spectral lines of the metal species radiate for a much longer duration and the electron density derived from these lines is expected to be smaller than the value deduced from H_α . The mean electron density values corresponding to the spectral line emission of the metal atoms

Table 2
Atomic mass m_a and ionization potential ϕ_{ion} of elements, relative abundance of minor elements (mass fractions) w_{minor} deduced from LIBS analysis of the potato skin and flesh. Assuming a typical composition of potatoes, the mass fractions w of the flesh were estimated in order to compare them to data reported in literature.

Element	m_a (a.m.u.)	ϕ_{ion} (eV)	w_{minor} (%)		w (ppm)	w (ppm) according to literature				
			Skin	Flesh		Flesh	Ref. [41]	Ref. [42]	Ref. [43]	Ref. [44]
Hydrogen	1.01	13.6	–	–	10%	–	–	–	–	–
Carbon	12.01	11.26	–	–	9.1%	–	–	–	–	–
Oxygen	16	13.62	–	–	79%	–	–	–	–	–
Nitrogen	14.01	14.55	–	–	0.3%	–	–	–	–	–
Magnesium	24.3	7.65	2.0	8.2	1300	300	210	2400	1200	1100
Aluminum	26.98	5.99	0.56	–	–	–	–	–	–	–
Calcium	40.08	6.11	2.2	1	170	150	70	51	–	–
Iron	55.85	7.9	0.86	0.13	20	10	7	7.8	20	23
Sodium	22.99	5.14	7.7	0.2	34	50	70	49	–	–
Manganese	54.94	7.43	0.05	–	–	1	–	1.7	5.6	6.8
Titan	47.88	6.82	0.09	–	–	–	–	–	–	–
Lithium	6.94	5.39	0.02	–	–	–	–	–	–	–
Silicon	28.09	8.15	39	–	–	–	–	–	–	–
Potassium	39.1	4.34	48	90.27	15000	5000	5300	6000	–	–
Copper	63.55	7.73	0.17	0.2	30	1.5	–	0.88	9.2	8.7

(see Figs. 4, 6 and 7) was estimated to about 1.8×10^{16} and $1.5 \times 10^{16} \text{ cm}^{-3}$ for ablation of the potato flesh and skin, respectively. These values have been used for the spectra calculations as they characterize the plasma zone where the emission of metal atoms originates from.

It is noted, that the measured electron density values are small and a decay from local thermal equilibrium may occur in the case of a plasma produced by laser ablation of organic materials. Organic elements have large energy gaps between the excitation levels and the establishment of LTE requires larger n_e -values according to the criterion of Griem [39]. Contrarily, metal atoms have many energy levels lying close to each other and a Boltzmann equilibrium distribution of their population number densities can be easily established. We expect therefore a

plasma in partial LTE, where the population number densities of metal species are determined by the equilibrium laws whereas a decay from the equilibrium distributions may occur for the organic species. However, the decay from equilibrium is expected to play a minor role in the present analysis as most of the plasma electrons originate from the ionization of metal atoms.

3.4. Evaluation of the relative concentrations of minor elements

Assuming a uniform plasma in local thermal equilibrium, the determination of the elemental composition is a problem of $k+1$ variables, the atomic number densities of k elements and the temperature. Here, the atomic number density n_X of an element X is the number of atoms per unit volume independently of the fact that the atoms are ionized or recombined to form a molecule. The k atomic number densities are equivalent to the total atomic number density $n_{\text{tot}} = \sum n_X$ and the $k-1$ relative elemental concentrations or mass fractions. Furthermore, the total number density can be substituted by the electron density that is measured via Stark broadening of spectral lines as illustrated in the previous section.

As the organic elements have much larger ionization potentials than the minor elements, the plasma electrons are mainly produced by the ionization of metal atoms in the temperature range $<8000 \text{ K}$. The determination of the concentrations of the most abundant metallic elements is thus crucial for the analysis. As the population number densities of the organic species may not reach the equilibrium distributions, the determination of the elemental concentrations of C, H, O and N was omitted.

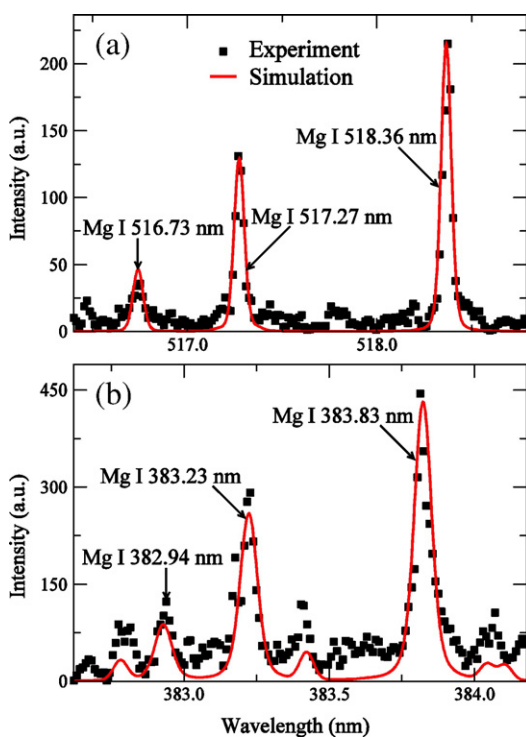


Fig. 4. Experimental spectra recorded during laser ablation of the potato skin and spectral radiance computed for a plasma in local thermal equilibrium. The spectral ranges (a) and (b) show two multiplets of magnesium having significantly different upper level energies. The relative intensities allowed for the measurement of the plasma temperature.

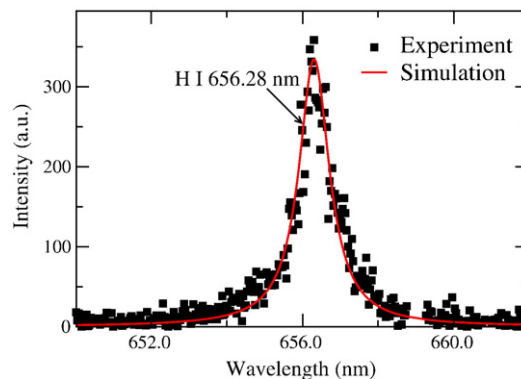


Fig. 5. Spectral shape of the H_{α} transition at 656.28 nm recorded during laser ablation of the potato skin. The electron density was estimated from the Stark broadening effect.

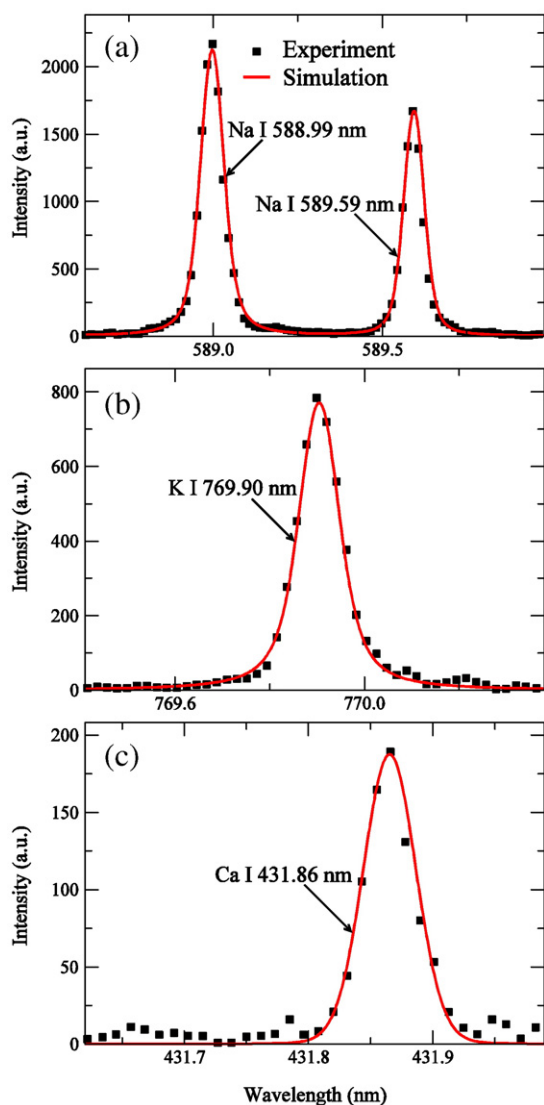


Fig. 6. Experimental spectra recorded during laser ablation of the potato skin and spectral radiance computed for a plasma in local thermal equilibrium. The sodium concentration was deduced from the self-absorption of the Na I 588.99 and 589.59 nm resonance lines (a). The potassium and calcium concentrations were deduced from the relative intensities of the selected lines presented in (b) and (c), respectively.

The calculation loop (see Fig. 2) was started with the previously estimated values of temperature and electron density and arbitrary mass fractions of elements. The elemental concentrations were then deduced by adjusting the relative intensities of the appropriate spectral lines. A fast convergence of the calculation loop is obtained by determining first the concentration of elements that significantly contribute to the production of electrons in the plasma. Thus, we adjusted first the concentrations of potassium, magnesium and calcium that have relatively large mass fractions in fresh vegetables. The corresponding spectral lines are displayed in Figs. 4, 6 (b) and (c). The concentrations of other minor elements were deduced afterwards using the same procedure. The spectral lines used for the determination of the concentrations of aluminum, lithium and silicon were shown in Fig. 7.

The resonance lines Na I 588.99 and 589.59 nm were significantly self-absorbed so that the intensity ratio $I_{588.99}/I_{589.59}$ was reduced with respect to the ratio expected for the optically thin case. As the calculation of spectral radiance takes into account the self-absorption, the good agreement between computed and measured spectra shown in Fig. 6(a) allowed us to verify that the applied procedure for the

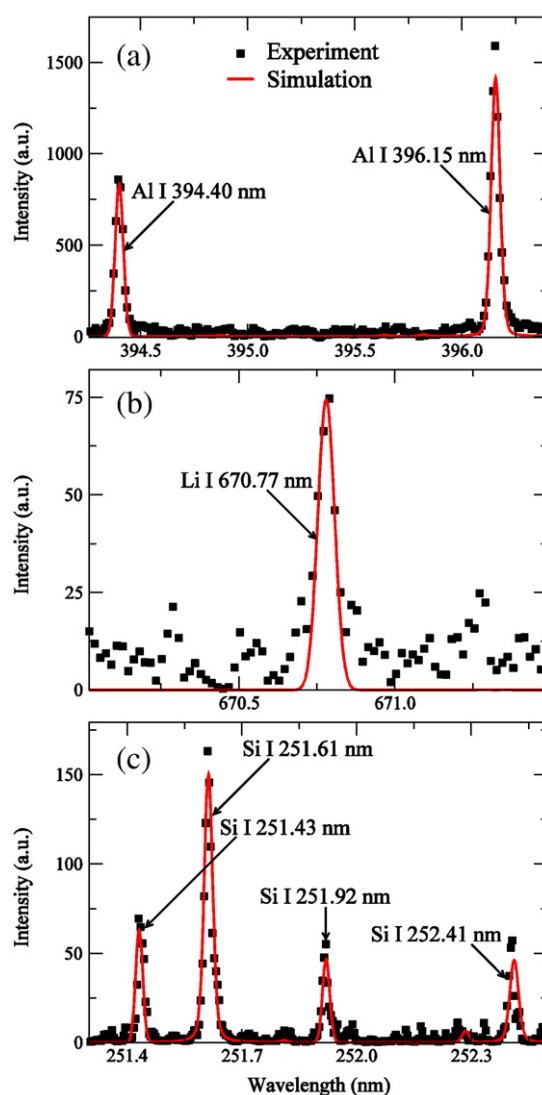


Fig. 7. Experimental spectra recorded during laser ablation of the potato skin and spectral radiance computed for a plasma in local thermal equilibrium. The aluminum, lithium and silicon concentrations were deduced from the relative intensities of the selected lines presented in (a), (b) and (c), respectively.

determination of elemental concentrations is valid. We note that the calculation was performed assuming a plasma diameter $L = 300 \mu\text{m}$ along the observation direction.

3.5. Elemental composition of potato skin and flesh

The elemental composition determined by the present analysis is displayed in Table 2 for the potato flesh and skin. All values are given in mass fractions. As mentioned above, the organic elements were not obtained by the LIBS measurements. We therefore present the relative mass fractions of the inorganic minor elements $w_m = M_X/M_{\text{inor}}$, where M_X is the mass per unit volume of element X and $M_{\text{inor}} = \sum_{\text{inor}} M_X$ is the mass per unit volume of all inorganic elements. Assuming a typical composition of organic elements in potatoes that contain about 77% water, 19% carbohydrates, 2% proteins, 0.1% lipids [41], we were able to estimate the absolute mass fractions of the minor elements $w = M_X/M_{\text{tot}}$ in the flesh. Here, $M_{\text{tot}} = \sum_{\text{all}} M_X$ is the total mass per unit volume of the potato.

The estimated mass fractions were compared to published data that were obtained using standard techniques for analysis of aliments (see Introduction). It is shown that the mass fractions of minor

inorganic elements measured for the potato flesh are close to the average mass fractions found in literature [41–44]. In particular, the order of abundance of the minor inorganic elements is in agreement with published data.

Comparing the composition measured for the flesh and skin, we note that magnesium and potassium have larger abundance in the flesh whereas the other minor elements have larger concentrations in the skin. The large mass fraction of potassium having the smallest ionization potential (see Table 2) may explain the larger electron density in the plasma produced by laser ablation of the flesh. In fact, due to the large abundance of potassium in the flesh, the overall number density of metal atoms in the plasma is larger than the value obtained for ablation of the skin. As the electrons are essentially generated by the ionization of metal atoms, the electron density is larger in the plasma produced by laser ablation of the flesh.

The elements Al, Mn, Ti, Li and Si were only detected for laser ablation of the potato skin. The mass fractions of elements in the flesh were found to be below the detection limits in our experiment that were estimated to about 0.5, 2, 3, 0.05 and 80, for Al, Mn, Ti, Li, and Si, respectively.

The evaluation of the measurement error is a difficult task. It depends on a large number of parameters. First of all, the applied LIBS analysis procedure does not include the mass fractions of the organic elements and therefore only determines the relative concentrations of the minor elements. The estimation of the absolute concentrations, that was done in order to compare the results with those reported in literature, was done by setting the total mass fraction of minor inorganic elements to a value typical for fresh potatoes. Thus, the systematic error of the mass fraction measurements on an absolute scale is large and may reach a factor of two. The uncertainties of the minor element relative concentrations depend critically on the energy gap between the upper energy levels of the spectral lines that have been chosen for the analysis. For example, a temperature variation of about 5% will cause a change of the intensity ratio of the Mg I 518.36 nm and K I 518.36 nm transitions of about 50%, whereas only 5% are expected for the Mg I 518.36 nm and Fe I 404.58 nm transitions as these lines have upper levels of similar energies. These uncertainties have to be added to the uncertainties of radiative decay ranging typically from 10 to 20% and the intensity measurement error. The latter critically depends on the signal-to-noise ratio and is large for concentrations close to the detection limit. In addition, the self-absorption of sodium tends to increase the measurement uncertainty of this element. Indeed, the optical thickness depends on the plasma density that is determined in procedure the via the electron density measurement. Consequently, the sodium measurement uncertainty depends on the uncertainty of n_e whereas the elemental concentrations measured with optically thin spectral lines only weakly depend on the electron density. In summary, the uncertainties of the minor element relative concentrations vary from a few % for optically thin lines of precisely known radiative decay with upper energy levels lying close to each others to values up to 100% in the worst case. An improvement of the measurement precision is possible by taking into account the spatial variation of temperature and plasma density.

3.6. Summary and conclusion

We have performed spectroscopic analysis of the plasma produced by laser ablation of potato flesh and skin using infrared radiation of 4 ns pulse duration. The emission spectra recorded with an Echelle spectrometer were compared to the spectral radiance computed for a plasma in local thermal equilibrium to deduce the mass fractions of the minor elements. The concentrations of organic elements were not measured as their population number densities are expected to decay from the Boltzmann equilibrium distributions. According to the moderate electron density $\approx 10^{16} \text{ cm}^{-3}$, only the metallic species were expected to have population number densities in agreement with the Boltzmann law.

In the temperature range of interest ($T=6500 \text{ K}$), the plasma electrons are essentially generated by the ionization of the metal atoms, and the possible decay from equilibrium of the organic species population densities has no significant influence on the deduced relative concentrations of the inorganic minor elements. Furthermore, as the calculation of the spectral radiance takes into account self-absorption of the spectral lines, the analysis procedure could be verified by measuring the optical thickness of the sodium resonance lines. In fact, the number density of sodium ground state atoms was found to have values that are large enough to change the relative intensities between the Na I 588.99 and 589.59 nm lines with respect to the intensity ratio in the optically thin case.

Comparing the mass fractions deduced from the present LIBS analysis of the potato flesh to values measured by ICP-AES, ICP-MS and AAS techniques, a good agreement was obtained for the detected minerals. In addition, significant differences were observed in the compositions of the potatoes flesh and skin. In particular, several elements such as Al, Mn, Ti, Li and Si were detected in the skin with relative concentrations from 0.02% for Li up to 39% for Si whereas the same elements had concentrations below the detection limit in the flesh.

Complementary investigations are planned in order to evaluate the possibility to include the organic elements in the LIBS measurement procedure and to validate the procedure on fresh vegetables of known composition.

Acknowledgement

The Algerian and the French Ministers of Higher Education and Scientific Research are acknowledged to support the present project.

References

- J.-C. Leblanc, T. Guérin, L. Noël, G. Calamassi-Tran, J.-L. Volatier, P. Verger, Estimated dietary exposure to principal food mycotoxins from The First French Total Diet Study, *Food Addit. Contam.* 22 (2005) 624–641.
- J.-C. Leblanc, Etude de l'alimentation totale française, Mycotoxines, minéraux et éléments traces, Report Institut National de la Recherche Agronomique, France, 2004.
- G. Miquel, Les effets des métaux lourds sur l'environnement et la santé, Rapport d'information n°261 fait pour le Sénat au nom de l'Office parlementaire d'évaluation des choix scientifique et technologique, 2001.
- G. Doner, A. Ege, Evaluation of digestion procedures for the determination of iron and zinc in biscuits by flame atomic absorption spectrometry, *Anal. Chem.* 520 (2004) 217–222.
- S. Saracoglu, K.O. Saygi, O.D. Uluozlu, M. Tuzen, M. Soyulak, Determination of trace element contents of baby foods from Turkey, *Food Chem.* 105 (2007) 280–285.
- M. Tuzen, M. Soyulak, Evaluation of trace element contents in canned foods marketed from Turkey, *Food Chem.* 102 (2007) 1089–1095.
- E.C. Lima, F. Barbosa, F.J. Krug, Lead determination in slurries of biological materials by ETAAS using a W-Rh permanent modifier, *Fresenius J. Anal. Chem.* 369 (2001) 496–501.
- D. Santos, F. Barbosa, A.C. Tomazelli, F.J. Krug, J.A. Nobrega, M.A.Z. Arruda, Determination of Cd and Pb in food slurries by GF AAS using cryogenic grinding for sample preparation, *Anal. Bioanal. Chem.* 373 (2002) 183–189.
- C.S. Kira, V.A. Maihara, Determination of major and minor elements in dairy products through inductively coupled plasma optical emission spectrometry after wet, partial digestion and neutron activation analysis, *Food Chem.* 100 (2007) 390–395.
- K.C. Chan, Y.C. Yip, H.S. Chu, High-throughput determination of seven trace elements in food samples by inductively coupled plasma-mass spectrometry, *J. AOAC Int.* 89 (2006) 469–479.
- Y. Sahan, F. Basoglu, S. Gucer, ICP-MS analysis of a series of metals (Namely: Mg, Cr, Co, Ni, Fe, Cu, Zn, Sn, Cd and Pb) in black and green olive samples from Bursa, Turkey, *Food Chem.* 105 (2007) 395–399.
- W. Lei, V. Motto-Ros, M. Boueri, Q. Ma, D. Zhang, L. Zheng, H. Zeng, J. Yu, Time-resolved characterization of laser-induced plasma from fresh potatoes, *Spectrochim. Acta Part B* 64 (2009) 891–898.
- A.W. Miziolek, V. Palleschi, in: Israel Schechter (Ed.), *Laser-Induced Breakdown Spectroscopy: Fundamental and Applications*, Cambridge University Press, 2006, Chapter 3.
- G.S. Senesi, M. Dell'Aglio, R. Gaudioso, A. De Giacomo, C. Zaccone, O. De Pascale, T.M. Miano, M. Capitelli, Heavy metal concentrations in soils as determined by laser-induced breakdown spectroscopy (LIBS), with special emphasis on chromium, *Environ. Res.* 109 (2009) 413–420.
- F. Colao, R. Fantoni, V. Lazic, A. Paolini, F. Fabbri, G.G. Ori, L. Marinangeli, A. Baliva, Investigation of LIBS feasibility for in situ planetary exploration: An analysis on Martian rock analogues, *Planet. Space Sci.* 52 (2004) 117–123.

- [16] V. Juvé, R. Portelli, M. Boueri, M. Baudelet, J. Yu, Space-resolved analysis of trace elements in fresh vegetables using ultraviolet nanosecond laser-induced breakdown spectroscopy, *Spectrochim. Acta Part B* 63 (2008) 1047–1053.
- [17] J.E. Carranza, B.T. Fisher, G.D. Yoder, D.W. Hahn, On-line analysis of ambient air aerosols using laser-induced breakdown spectroscopy, *Spectrochim. Acta Part B* 56 (2001) 851–864.
- [18] Ann Brysbaert, Krystalia Melessanaki, Demetrios Anglos, Pigment analysis in Bronze Age Aegean and Eastern Mediterranean painted plaster by laser-induced breakdown spectroscopy (LIBS), *J. Archaeol. Sci.* 33 (2006) 1095–1104.
- [19] D. Body, B.L. Chadwick, Optimization of the spectral data processing in a LIBS simultaneous elemental analysis system, *Spectrochim. Acta Part B* 56 (2001) 725–736.
- [20] J. Hermann, Système et procédé d'analyse quantitative de la composition élémentaire de la matière par spectroscopie du plasma induit par laser (LIBS). Patent, PCT-FR2009-001221.
- [21] L.C. Green, P.P. Rush, C.D. Chandler, Oscillator strengths and matrix elements for the electric dipole moment for hydrogen, *Astrophys. J.* (1957) 37 Suppl 3.
- [22] D. Stuck, B. Wende, Measurement of transition probabilities of C I multiplets in the visible and vacuum-ultraviolet spectral region utilizing arc-plasma emission and synchrotron-calibrated radiometric transfer standards, *Phys. Rev. A* 9 (1974) 1–8.
- [23] W.L. Wiese, M.W. Smith, B.M. Glennon, *Atomic Transition Probabilities*, vol. I, U.S. Government Printing Office, Washington, D.C., 1966, NSRDS-NBS 4.
- [24] E.M. Anderson, V.A. Zilitis, E.S. Sorokina, Semiempirical calculation of the oscillator strengths of the magnesium atom, *Opt. Spectr.* 23 (1967) 102.
- [25] G. Tachiev and C. Froese Fischer, http://www.vuse.vanderbilt.edu/~cff/mchf_collection/ (MCHF, energy adjusted, downloaded on Dec. 10, 2003).
- [26] W.H. Smith, H.S. Liszt, Absolute oscillator strengths for some resonance multiplets of Ca I, II, Mg I, II, B I, and Al I, *J. Opt. Soc. Am.* 61 (1971) 938.
- [27] W.L. Wiese, M.W. Smith, B.M. Miles, *Atomic Transition Probabilities*, vol. II, U.S. Government Printing Office, Washington, DC, 1969, NSRDS-NBS 22.
- [28] R.L. Kurucz, in: M. McNally (Ed.), *Semiempirical calculation of gf values for the iron group*, *Trans. IAU, XXB*, Kluwer, Dordrecht, 1988, pp. 168–172.
- [29] J.R. Fuhr, G.A. Martin, W.L. Wiese, Atomic transition probabilities-iron through nickel, *J. Phys. Chem. Ref. Data* 17 (1988).
- [30] G.A. Martin, J.R. Fuhr, W.L. Wiese, Atomic transition probabilities—scandium through manganese, *J. Phys. Chem. Ref. Data* 17 (1988).
- [31] T. Garz, Absolute oscillator strengths of Si I lines between 2500 Å and 8000 Å, *Astron. Astrophys. A&A* 26 (1973) 471.
- [32] A. Bielski, A critical survey of atomic transition probabilities for Cu I (102 lines), *JQSRT* 15 (1975) 463.
- [33] A. Lesage, Experimental Stark widths and shifts for spectral lines of neutral and ionized atoms. A critical review of selected data for the period 2001–2007, *New Astron. Rev.* 52 (2009) 471–535.
- [34] N. Konjević, W.L. Wiese, Experimental Stark widths and shifts for spectral lines of neutral and ionized atoms (a critical review of selected data for the period 1983 through 1988), *J. Phys. Chem. Ref. Data* 19 (1990) 1307–1385.
- [35] N. Konjević, J.R. Roberts, A critical review of the Stark widths and shifts of spectral lines from non-hydrogenic atoms, *J. Phys. Chem. Ref. Data* 5 (1976) 209–257.
- [36] S. Bukvić, S. Djeniže, A. Srečković, Measured Stark parameters of the NaI-D spectral lines in argon plasma, *Publ. Obs. Astron. Belgrade No.*, 50, 1995, pp. 35–38.
- [37] N. Konjević, A. Lesage, J.R. Fuhr, W.L. Wiese, Experimental Stark widths and shifts for spectral lines of neutral and ionized atoms (a critical review of selected data for the period 1989 through 2000), *J. Phys. Chem. Ref. Data* 31 (2002) 919–927.
- [38] J. Hermann, C. Dutouquet, Local thermal equilibrium plasma modeling for analyses of gas-phase reactions during reactive-laser ablation, *J. Appl. Phys.* 91 (2002) 10188–10193.
- [39] H.R. Griem, *Plasma Spectroscopy*, McGraw-Hill, New York, 1964.
- [40] J. Hermann, C. Boulmer-Leborgne, D. Hong, Diagnostics of the early phasis of an ultraviolet laser-induced plasma by spectral line analysis considering self-absorption, *J. Appl. Phys.* 83 (1998) 691–696.
- [41] L. Randoin, P. Le Gallic, Y. Dupuis, A. Bernardin, *Tables de composition des aliments*, Editions Jacques Lanore, 2004, p. 70.
- [42] J.-C. Favier, J. I-Ripert, C. Toque, M. Feinberg, *Répertoire général des aliments: Tables de composition*, Ciqual-Regal, 1995, p. 577.
- [43] R.C. Rivero, P.S. Hernández, E.M.R. Rodríguez, J.D. Martín, C.D. Romero, Mineral concentrations in cultivars of potatoes, *Food Chem.* 83 (2003) 247–253.
- [44] F. Di Giacomo, A. Del Signore, M. Giaccio, Determining the geographic origin of potatoes using mineral and trace element content, *J. Agric. Food Chem.* 55 (2007) 860–866.